Published in final edited form as:
Virology. 2005 September 30; 340(2): 245–254.

Acute respiratory infection with mouse adenovirus type 1

Jason B. Weinberg[a,*], **Gregory S. Stempfle**[a], **John E. Wilkinson**[b], **John G. Younger**[c], and **Katherine R. Spindler**[d]

a *University of Michigan Health System, Division of Pediatric Infectious Diseases, Department of Pediatrics, L2225 Women's/0244, 1500 East Medical Center Drive, Ann Arbor, MI 48109-0244, USA*

b *University of Michigan, Department of Pathology and Unit for Laboratory Animal Medicine, 018 ARF, 1500 West Medical Center Drive, Ann Arbor, MI 48109-0614, USA*

c *University of Michigan, Department of Emergency Medicine, B1354 Taubman Center, 1500 East Medical Center Drive, Ann Arbor, MI 48109-0303, USA*

d *University of Michigan, Department of Microbiology and Immunology, 6724 Medical Sciences Building II, 1150 West Medical Center Drive, Ann Arbor, MI 48109-0620, USA*

Abstract

Studies of the pathogenesis of adenovirus respiratory disease are limited by the strict species-specificity of the adenoviruses. Following intranasal inoculation of adult C57BL/6 mice with mouse adenovirus type 1 (MAV-1), we detected MAV-1 early region 3 (E3) and hexon gene expression in the lungs at 7 days post-infection (dpi). We detected MAV-1 E3 protein in the respiratory epithelium 7 dpi. We did not detect viral mRNA or protein at 14 dpi, but MAV-1 DNA was detected by PCR at 21 dpi. Chemokine transcript levels increased between 7 and 14 dpi in the lungs of infected mice. MAV-1 infection induced a patchy cellular infiltrate in lungs at 7 and 14 dpi. This is the first report demonstrating the presence of MAV-1 in the respiratory epithelium of infected mice and describing chemokine responses in the lung induced by MAV-1 respiratory infection. MAV-1 infection of mice has the potential to serve as a model for inflammatory changes seen in human adenovirus respiratory disease.

Keywords

Adenovirus; Chemokine; Lung; Inflammation

Introduction

Human adenoviruses cause a wide range of upper and lower respiratory tract infections in children (Carballal et al., 2002; Edwards et al., 1985; Larranaga et al., 2000; Pacini et al., 1987). Adenoviruses are also a common cause of upper respiratory tract infection and pneumonia in military recruits (Huebner et al., 1958; Kolavic-Gray et al., 2002; Mogabgab, 1968). Immunocompromised patients experience greater problems due to adenovirus infections, including more aggressive respiratory infections, transplant loss and death (Kojaoghlanian et al., 2003). A potential long-term consequence of persistent adenovirus infection is an increased risk for the development of asthma and chronic obstructive pulmonary disease (COPD) (Hogg, 1999, 2001). Human adenoviruses are also significant as vectors for in vitro and in vivo delivery of genes into mammalian cells (reviewed in Kay et al., 2001).

* Corresponding author. Fax: +1 734 936 7635..
*E-mail addresses:*jbwein@umich.edu (J.B. Weinberg),stempfle@umich.edu (G.S. Stempfle),jerby@umich.edu (J.E. Wilkinson),jyounger@umich.edu (J.G. Younger),krspin@umich.edu (K.R. Spindler).

Chemokines are chemotactic cytokines that serve as chemoattractants for cells involved in the inflammatory response to stimuli such as infection (Luster, 1998; Rollins, 1997; Taub, 1996). Combined in vitro, ex vivo and in vivo data suggest that both intact (Alcorn et al., 2001; Booth et al., 2004; Harrod et al., 1998; Kajon et al., 2003; Leland Booth and Metcalf, 1999; Otake et al., 1998) and replication-deficient (Amin et al., 1995; Kodama et al., 2001; Noah et al., 1996; Schwarz et al., 1999) human adenoviruses are capable of inducing chemokine responses in human, murine and bovine lung. Chemokines potentially play a significant role in the pathophysiology of asthma (Blease et al., 2000; Lukacs, 2001) and COPD (Beeh et al., 2003; Qiu et al., 2003; Saetta et al., 2002; Traves et al., 2002). Chemokine responses to adenovirus vectors contribute to difficulties encountered with limited persistence of the vector in its host, low levels of expression of desired genes and potential morbidity associated with use of the vector (reviewed in Liu and Muruve, 2003).

A variety of models have been used to study chemokine responses to adenovirus infection. In vitro systems have used infection of cell lines with adenovirus or transduction with adenovirus vectors (Alcorn et al., 2001; Kodama et al., 2001; Leland Booth and Metcalf, 1999; Schwarz et al., 1999). An ex vivo lung slice model has been used to examine chemokine responses to adenovirus infection in the context of a relevant tissue (Booth et al., 2004). The majority of these studies have focused on upregulation of interleukin 8 (IL-8), a CXC chemokine that serves as a major neutrophil chemoattractant and activator (Baggiolini et al., 1994). Relatively few studies have used in vivo animal models to examine chemokine responses to respiratory infection with human adenovirus (Harrod et al., 1998; Kajon et al., 2003). In vivo studies of human adenovirus pathogenesis are limited by the strict species-specificities of the adenoviruses. Because exposure of mice to human adenovirus does not result in a fully permissive infection (Ginsberg et al., 1991; Kajon et al., 2003), this system does not allow for a complete assessment of host inflammatory responses to persistent adenovirus infection. Human adenovirus infection of cotton rats (*Sigmodon hispidus*) has shown the most promise as an animal model of human adenovirus respiratory disease (Pacini et al., 1984; Prince et al., 1993), but it depends on infection with a high dose of a virus that is not fully adapted to the host. This drawback is particularly relevant in the study of links between adenovirus infection and chronic lung disease such as asthma or COPD, which are more likely to be associated with effects of persistent rather than acute infection.

Mouse adenovirus type 1 (MAV-1) serves as an excellent animal model system for studying adenovirus pathogenesis, providing the means to define viral and host factors involved in both acute and persistent adenovirus infections (reviewed in Smith and Spindler, 1999). The MAV-1 virion is structurally similar to that of human adenoviruses (Wigand et al., 1977), and its genomic organization is also similar to that of human adenovirus (Meissner et al., 1997). With the exception of the early region 3 (E3) gene (Beard et al., 1990), MAV-1 gene products have sequence similarity to those of human adenoviruses (Ball et al., 1988, 1989, 1991; Beard et al., 1990; Cauthen and Spindler, 1996; Kring et al., 1992; Kring and Spindler, 1990). Of particular interest, given the potential association between the human adenovirus early region 1A (E1A) gene and long-term sequelae of infection such as COPD (Elliott et al., 1995; Matsuse et al., 1992), MAV-1 E1A has approximately 40% similarity to human adenovirus E1A, with the strongest similarity in conserved region 2 (CR2) (Ball et al., 1988). MAV-1 E1A shares functional roles of human adenovirus E1A, binding to the mouse cellular proteins, retinoblastoma protein and pRb-related protein (Fang et al., 2004; Smith et al., 1996) and transactivating the human adenovirus type 5 E3 promoter (Ball et al., 1988).

Few studies directly address respiratory infection with MAV-1 or the role of chemokine responses to MAV-1. Following intraperitoneal (i.p.) MAV-1 inoculation of adult C57BL/6 mice, increased mRNA levels for the chemokines IP-10, MCP-1 and TCA-3 were detected in the brain between 3 and 4 days post-infection (dpi) (Charles et al., 1999). MAV-1 organ tropism

following intranasal (i.n.) inoculation of outbred mice is similar to that observed following i.p. inoculation (Kajon et al., 1998). In each case, virus was identified in multiple organs including lung, spleen and brain (Kajon et al., 1998). Following i.n. inoculation of newborn BALB/c mice less than 24 h old, peribronchiolar infiltrates comprised of macrophages, and lymphocytes were noted 3 dpi (Gottlieb and Villarreal, 2000).

We and others have used mouse models to study the chemokine responses to respiratory infections with a variety of viruses, including acute viral infections with respiratory syncytial virus (Domachowske et al., 2000; Haeberle et al., 2001; John et al., 2003; Mejias et al., 2004; Miller et al., 2004; Power et al., 2001; Tekkanat et al., 2002) and influenza virus (Dawson et al., 2000; Tumpey et al., 2000) as well as persistent viral infections such as those caused by murine gammaherpesvirus 68 (Sarawar et al., 2002; Weinberg et al., 2002, 2004). In this study, we demonstrate that respiratory infection is established following i.n. inoculation of C57BL/6 mice with MAV-1. Respiratory infection with MAV-1 results in chemokine upregulation and cellular inflammation in the lung. These data indicate that respiratory infection with MAV-1 may serve as a useful model to study adenovirus respiratory disease.

Results

Clinical signs of MAV-1 infection

In order to study MAV-1 respiratory infection, we inoculated 4- to 6-week-old C57BL/6 mice i.n. with 10^5 plaque-forming units (PFU) of MAV-1 and carefully monitored them until 14 dpi. At no time point did mice infected with MAV-1 exhibit clinical signs suggesting respiratory distress such as tachypnea or labored respirations. CNS symptoms such as ataxia, hyperreflexia, hyper-esthesia, paresis and flaccid paralysis were absent in all infected mice.

Detection of MAV-1 in the lung

Using in situ hybridization, Kajon et al. (1998) demonstrated the presence of MAV-1 in the lungs of adult outbred mice following both i.n. and i.p. inoculation. We sought to confirm and expand on these findings in the current study using inbred mice. In three separate experiments (n = 2 to 6 mice per condition at each time point), we harvested total RNA from lungs of mice at 1, 4, 7 and 14 dpi. We used ribonuclease protection assay (RPA) to detect the expression of MAV-1 E3 and hexon genes in the lung at each time point. We did not detect E3 gene expression at 1 or 4 dpi (data not shown). We detected E3 gene expression in 4 of 6 mice at 7 dpi (Fig. 1A) but did not detect E3 gene expression in any mice at 14 dpi. Expression of the late gene encoding the structural protein, hexon, was also detected at 7 dpi but not at 14 dpi in the lungs of infected mice (Fig. 1A). Paralleling these data, we found evidence of infectious virus in lung homogenates at 7 dpi but not at 14 dpi by plaque assay titration on mouse 3T6 fibroblast monolayers (data not shown). As expected, we did not detect E3 or hexon gene expression in the lungs of mock-infected animals at any time point (Fig. 1A).

MAV-1 has a tropism for endothelial cells in the CNS and other organs (Charles et al., 1998; Guida et al., 1995; Kajon et al., 1998; Moore et al., 2003). To determine whether MAV-1 is capable of infecting respiratory epithelial cells following i.n. inoculation, we performed immunohistochemistry on paraffin-embedded sections of lungs harvested at various time points following infection to localize MAV-1 E3 protein. At 7 dpi, virus-specific staining was evident in respiratory epithelial cells lining the medium and large airways of the lung (Fig. 2). At 14 dpi, MAV-1-specific staining was not present in respiratory epithelial cells of infected lungs, although there was occasional staining of vascular endothelial cells in the lung (arrow, Fig. 2). No staining was noted using preimmune rabbit serum as a primary antibody (data not shown).

Expression of hexon and E3 genes was not detected in lungs harvested from a separate group of mice at 21 dpi (data not shown). However, we detected the presence of MAV-1 DNA in the lungs of 2 of 3 mice at 21 dpi by PCR (Fig. 1B). Together, these data suggest that i.n. inoculation with MAV-1 resulted in a productive pulmonary infection in C57BL/6 mice involving respiratory epithelial cells. Following acute infection, MAV-1 genome persisted in the lung in the absence of detectable viral gene expression.

Chemokine responses to MAV-1 infection

Chemokine upregulation induced by MAV-1 has been described in the CNS but not the lung following i.p. inoculation (Charles et al., 1999). We used RPA to quantify chemokine gene expression in the lungs of mice infected i.n. with MAV-1. Data from a representative experiment are presented in Fig. 3. Prior to infection or at 1 and 4 dpi, we noted little chemokine expression in the lungs of mice, and levels of chemokine expression did not differ between MAV-1-infected and mock-infected mice (data not shown). In contrast, MAV-1 infection upregulated the expression of nearly all chemokine genes measured at later time points relative to mock infection (Fig. 3A). Levels of expression of IP-10 and Ltn peaked at 7 dpi, while levels of expression of MIP-1α, MIP-1β and RANTES peaked at 14 dpi. MCP-1 and TCA-3 expression was increased in MAV-1-infected animals to similar levels at 7 and 14 dpi. No significant differences in MIP-2 expression between MAV-1-infected and mock-infected mice were detected at any time point. Expression of the eotaxin gene was not reliably detected by RPA in lungs of MAV-1-infected or mock-infected mice at any time point (data not shown). Similar RPA results were obtained in separate experiments from infected mice at identical time points (data not shown).

To verify that altered levels of chemokine gene expression after infection were reflected in chemokine protein levels, we measured RANTES protein levels in lung homogenates at 7 and 14 dpi (Fig. 3B). At 7 dpi, levels of RANTES protein were not increased in the lungs of infected compared to mock-infected mice. At 14 dpi, when RANTES gene expression was dramatically upregulated in the lungs of infected mice (Fig. 3A), levels of RANTES protein were also significantly elevated compared to mock-infected mice (Fig. 3B).

Cellular inflammatory responses to MAV-1 infection in the lung

Chemokines are chemotactic cytokines that form a concentration gradient to attract cells involved in the inflammatory response to pathogens and other stimuli (Luster, 1998). Based on the chemokine upregulation we detected in the lungs and brains of infected mice, we predicted that a cellular inflammatory response would accompany MAV-1 respiratory infection. To assess cellular inflammation, we examined hematoxylin and eosin-stained sections of lungs and brain from MAV-1-infected and mock-infected mice. No cellular infiltrate was present in the lungs of mock-infected mice at any time point (Fig. 4A) or in the lungs of infected mice at 1 and 4 dpi (data not shown). A mild patchy interstitial pneumonitis was present in lungs of infected mice at both 7 and 14 dpi (Fig. 4A) that was characterized by a predominantly mononuclear infiltrate and thickened alveolar walls. In addition, scattered areas of hypercellularity were focused around medium and large airways in the lungs of infected mice at 7 dpi; these areas consisted predominantly of mononuclear cell infiltrates. These changes were also seen, though to a lesser extent, at 14 dpi. Thus, maximum cellular inflammation in the lung was present at 7 dpi when virus was detected in the lung by RPA, immunohistochemistry and plaque assay and was reduced when virus had been cleared from the lung at 14 dpi.

In a separate experiment, we used bronchoalveolar lavage (BAL) to characterize the airway cellular inflammatory response to MAV-1 respiratory infection at 7 dpi, when the greatest amount of cellular inflammation was noted in the lungs (Fig. 4B). BAL fluid from mock-

infected animals had a monotonous population of alveolar macrophages. These cells were also evident in BAL fluid from MAV-1-infected animals. In addition, BAL fluid from infected animals contained a variable degree of neutrophils (open arrow, Fig. 4B), ranging from 1.5% to 28.3% of the total population of cells (Fig. 4C). In contrast, BAL fluid from mock-infected animals contained only between 0.3% and 0.5% neutrophils. Only rare leukocytes of other types were noted in either mock-infected or MAV-1-infected animals, and their percentages did not differ among groups (data not shown).

Discussion

We demonstrate here that MAV-1 is capable of establishing a respiratory infection in the lungs of C57BL/6 mice and describe the novel finding that MAV-1 protein is present in respiratory epithelial cells following i.n. inoculation. We observed a parallel between viral gene expression and chemokine upregulation in the lungs. As expected from the chemokine upregulation we detected, MAV-1 infection in the lung elicited a cellular inflammatory response that resulted in an interstitial pneumonitis and foci of inflammation around larger airways.

Previous work from our laboratory showed that MAV-1 DNA could be detected using in situ hybridization in the lung following both i.n. and i.p. inoculation of NIH Swiss outbred mice with MAV-1, but its distribution was limited to the vascular endothelium (Kajon et al., 1998). Here, we found MAV-1 protein in both vascular endothelium and respiratory epithelium following i.n. inoculation of C57BL/6 mice. Several possibilities may explain the apparent difference in cell tropism. The lack of detection of MAV-1 nucleic acid in the earlier report is possibly due to a lower viral dose, 10^3 PFU, versus 10^5 PFU used here. The higher dose may increase the efficiency of entry into a cell. Following virus entry, the higher dose may result in increased viral replication to levels whereby viral protein is detectable by immunohistochemistry. We believe that a less likely explanation is that detection of protein in respiratory epithelial cells using immunohistochemistry was more sensitive than detection of MAV-1 DNA by in situ hybridization.

Another possibility explaining the apparent cell tropism difference between this study and the previous study (Kajon et al., 1998) is that different mouse strains were used, C57BL/6 and NIH Swiss outbred mice, respectively. Differential host susceptibility to MAV-1 infection is seen among various inbred and outbred mouse strains (Guida et al., 1995; Kring et al., 1995; Spindler et al., 2001). The 50% lethal dose (LD_{50}) for outbred NIH Swiss outbred mice is 17 PFU (Kring et al., 1995), much lower than the LD_{50} of $>10^{4.4}$ PFU for C57BL/6 mice (Spindler et al., 2001). The underlying basis for these differences in susceptibility is unknown but is likely to involve mouse strain-specific differences in immune responses to MAV-1. For instance, chemokine responses to MAV-1 infection in the brain differ between C57BL/6 and BALB/c mice (Charles et al., 1999). It is therefore possible that our ability to detect MAV-1 in the respiratory epithelium in the present study and not in our previous study (Kajon et al., 1998) is based on differing abilities of the two mouse strains to efficiently prevent or control viral infection in respiratory epithelial cells.

Histopathologic descriptions of adenovirus respiratory disease in humans are quite limited and largely include descriptions of fatal disease and disease in immunocompromised individuals (Becroft, 1967, 1971; Chany et al., 1958; Zahradnik et al., 1980). MAV-1-induced respiratory disease in C57BL/6 mice appears to share some characteristics with human disease. The respiratory epithelium appears to be involved in both cases, although the significant epithelial damage seem in some human cases (Becroft, 1967, 1971; Chany et al., 1958) was not prominent in this study. Histopathologic features of respiratory disease induced by MAV-1 are also similar in some ways to those present in the cotton rat model of human adenovirus type 5 (Prince et al., 1993), including the presence of viral antigen in respiratory epithelial cells and a cellular

infiltrate of peribronchiolar regions that was most pronounced at 7 dpi in each case. MAV-1 infection of C57BL/6 mice resulted in a patchy interstitial pneumonitis (Fig. 4A); an early intra-alveolar cellular exudate, which was comprised predominantly of macrophages and polymorphonuclear leukocytes in the cotton rat model (Prince et al., 1993), was present following MAV-1 infection, although to a lesser extent than in human adenovirus infection of cotton rats. Although the riboprobe template used to measure chemokine gene expression in this report includes fewer CXC than CC chemokines, it is perhaps notable that MIP-2, a CXC chemokine, was the only chemokine detected that was not upregulated following MAV-1 infection. MIP-2 serves as a potent neutrophil chemoattractant in lung injury (reviewed in Guo and Ward, 2002), and the absence of MIP-2 upregulation in the setting of MAV-1 respiratory infection in part may explain the less prominent neutrophil influx into the airways in the present report.

Adenoviruses are capable of establishing persistent infections in their hosts (reviewed in Horwitz, 2001). Persistent adenovirus infection may contribute to chronic lung disease. The human adenovirus E1A protein is expressed in airway epithelial cells and type 2 alveolar cells in human lung tissue (Elliott et al., 1995). Human adenovirus E1A DNA was detected more often in lung tissue from patients with COPD than in tissue from control subjects (Matsuse et al., 1992). Human adenovirus DNA was isolated more frequently in the lungs of children with asthma than in healthy children (Marin et al., 2000). Adenovirus capsid protein was detected in BAL fluid of children with steroid-resistant asthma but not in children without persistent asthma (Macek et al., 1994). In a guinea pig model, persistent human adenovirus infection was associated with chronic lung inflammation (Vitalis et al., 1996), enhanced inflammatory response to cigarette smoke exposure (Vitalis et al., 1998) and lung destruction following chronic cigarette smoke exposure (Meshi et al., 2002). In addition, persistent adenovirus infection of guinea pigs modifies steroid responsiveness to ovalbumin-induced allergic lung disease (Yamada et al., 2000), potentially by inhibiting AP-1-mediated effects of steroid on the expression of the chemokines eotaxin and MCP-1 (Yamada et al., 2002).

Persistent MAV-1 infections have also been documented (reviewed in Smith and Spindler, 1999). In mice infected with MAV-1, high titers of virus were found in the urine for up to 24 months (van der Veen and Mes, 1973) and in the liver up to 52 dpi (Wigand, 1980). Using PCR amplification and in situ hybridization, Smith et al. demonstrated persistence of viral DNA in the brain, spleen, kidneys and lymph nodes of NIH Swiss outbred mice for up to 55 weeks following i.p. inoculation of MAV-1 (Smith et al., 1998). We detected MAV-1 DNA in the lungs of infected mice at 21 dpi using PCR (Fig. 1B). Using nested PCR to amplify a portion of the MAV-1 E1A coding sequence, we have also detected MAV-1 genome in the lungs of infected BALB/c mice at 44 dpi (data not shown). MAV-1 therefore has the potential to serve as a powerful tool to study the role of persistent adenovirus infection in chronic lung disease.

It is clear from the data presented in this report that i.n. inoculation of C57BL/6 mice results in an acute respiratory infection. Given the availability of multiple transgenic and knockout mouse strains together with mutant MAV-1 deficient in the production of E1A (Smith et al., 1996) or E3 proteins (Beard and Spindler, 1996; Cauthen et al., 1999), MAV-1 infection will allow the study of specific host inflammatory responses and specific viral genes involved in the pathogenesis of adenovirus-induced respiratory infection.

Materials and methods

Viruses, mice and experimental infections

Wild-type MAV-1 was grown and passaged in NIH 3T6 fibroblasts, and titers of viral stocks were determined by plaque assay on 3T6 cells as previously described (Cauthen and Spindler,

1999). Four- to six-week-old male C57BL/6J mice were purchased from Harlan and maintained in microisolator cages. Under light isoflurane anesthesia, mice were inoculated i.n. with 10^5 PFU in 20 μl sterile PBS. Control mice were inoculated i.n. with conditioned media at an equivalent dilution in PBS. Mice were euthanized at the indicated time points. Organs were harvested, snap frozen in a dry ice and ethanol bath and stored at −20 °C until processed further. All animal work complied with all relevant federal and institutional policies.

Histology

In a subset of mice, lungs and brain were harvested and fixed in 10% formalin. Prior to fixation, lungs were gently inflated with PBS via the trachea to maintain lung architecture. After fixation, organs were embedded in paraffin, and 5 μm sections were cut for histopathology and immunohistochemistry. Sections were stained with hematoxylin and eosin to evaluate cellular infiltrates. All sectioning and staining was performed by the University of Michigan Department of Pathology Histology Research Laboratory.

Immunohistochemistry

Sections were deparaffinized in Citri-solv (Fisher) and rehydrated in sequential ethanol baths (100%, 95% and 75% ethanol for 5 min each) followed by a PBS wash (10 min). Antigen retrieval was accomplished using sequential washes in 100 mM Tris–HCl, pH 10, boiling in a microwave oven (4 washes, 5 min each). Slides were allowed to cool gradually to room temperature and were then washed twice in phosphate-buffered saline (PBS). Endogenous peroxidase activity was quenched with hydrogen peroxide, and slides were blocked by incubating with horse serum (1:667 in PBS). MAV-1 protein was detected using αE3-1 antiserum (Beard and Spindler, 1995) diluted 1:2000 in blocking buffer. This polyclonal rabbit antiserum was raised against a GST fusion protein containing the unique amino acid sequence from the E3 gp11K protein. Rabbit preimmune serum was used as a negative control. The secondary antibody was biotinylated anti-rabbit antibody (Vectastain ABC Kit, Vector Laboratories). Detection was accomplished using the Peroxidase Substrate Kit (Vector Laboratories) according to the manufacturer's instructions. Slides were counterstained for 5 min with hematoxylin.

Bronchoalveolar lavage

Airspace inflammatory cells were collected by BAL. Lungs of euthanized animals were lavaged three times with 0.8 ml phosphate-buffered saline. Cells in the BAL fluid were pelleted by centrifugation, cytospun onto glass slides and stained with hematoxylin and eosin. Cells from ten randomly selected high-power fields were counted on each slide, and the proportion of different leukocyte subtypes calculated.

Isolation of RNA and DNA

The left lung was homogenized with sterile glass beads and 1 ml TRIzol Reagent (Gibco-BRL) using a Mini Beadbeater (Biospec Products). The homogenates were incubated at room temperature for 10 min, and then 200 μl of chloroform was added to each sample. Following a 3-min incubation at room temperature, the tubes were centrifuged at 12,000 ×*g* for 15 min at 4 °C. The aqueous phase was transferred to a new microcentrifuge tube, and total RNA was precipitated with isopropanol. DNA was extracted from approximately one-third of the right lung using the DNeasy Tissue Kit (Quiagen Inc.) according to the manufacturer's protocol.

Ribonuclease protection assays

Total RNA was analyzed by RPA to measure viral, chemokine and cytokine gene expression as previously described (Rochford et al., 2001; Weinberg et al., 2002). The RPAs are performed in probe excess, so they give a quantitative measure of the specific RNAs present. Expression

of murine chemokines and cytokines was measured using the mCK-5c riboprobe template (PharMingen). An MAV-1 E3 probe was prepared from plasmid pZU14 as described (Fang et al., 2004). The full-length E3 template measured 714 nucleotides (nt), and the size of the protected fragment was 645 nt. A genomic MAV-1 hexon probe was prepared from plasmid pHEX as described (Fang et al., 2004). The full-length hexon template measured 395 nt, and the size of the protected fragment was 337 nt. The templates for internal β-actin (Fang et al., 2004) and L32 (Hobbs et al., 1993) controls were previously described. Linearized E3 and β-actin templates were combined in equimolar concentrations for use in riboprobe syntheses driven by T3 bacteriophage RNA polymerase. Linearized MAV-1 hexon and L32 templates combined in equimolar concentrations for use in riboprobe syntheses were driven by T7 bacteriophage RNA polymerase. All syntheses used [α-^{32}P]UTP (Amersham) as the labeling nucleotide. Probe bands were visualized by autoradiography and were quantified where indicated using the Storm PhosphorImager and ImageQuant software (Molecular Dynamics).

PCR amplification of MAV-1 E1A

DNA extracted from the lungs of mice was amplified using PCR to detect the presence of MAV-1 E1A. 80 ng of DNA was amplified by PCR in a reaction volume of 20 μl containing 4 μl of 5× GoTaq Reaction Buffer (Promega, final concentration 1.5 mM $MgCl_2$), 0.5 U GoTaq DNA polymerase (Promega), 0.2 mM dNTPs and 150 ng each of E1A-FO1 (5′ ATG TCG CGG CTC CTA CG 3′) and E1A-RE1 (5′ CAA CGA ACC ATA AAA AGA CAT CAT 3′). The PCR amplification was carried out for 35 cycles at an annealing temperature of 50 °C. Amplified products were separated on a 1.8% agarose gel, stained with ethidium bromide and photographed using an Electrophoresis Documentation and Analysis System (Kodak).

Measurement of chemokine protein

Protein levels of the murine chemokine RANTES were measured in supernatants from organ homogenates obtained as described above. Specific chemokines were quantified using a standard method of sandwich ELISA as previously described (Hogaboam et al., 1998; Walley et al., 1997). In brief, microtiter plates were coated with the appropriate chemokine capture antibody. Samples were added to wells for 1 h at 37 °C. Recombinant murine chemokine standard curves were used to calculate the chemokine concentrations. Detection and processing were performed with the appropriate biotinylated polyclonal rabbit anti-cytokine antibody (3.5 μg/ml), streptavidin–peroxidase conjugate (Bio-Rad) and chromogen substrate (Bio-Rad). Plates were read on an ELISA plate scanner at 492 nm.

Acknowledgements

We thank Pamela Lincoln for her expert assistance in performing chemokine ELISA assays. We also thank Mike Imperiale, John Younger and Tom Shanley for comments on the manuscript. J.B.W. was supported by a Janette Ferrantino Award from the University of Michigan Department of Pediatrics and by NICHD grant HD28820. K.R.S. was supported by NIH R01 AI023762.

References

Alcorn MJ, Booth JL, Coggeshall KM, Metcalf JP. Adenovirus type 7 induces interleukin-8 production via activation of extracellular regulated kinase 1/2. J Virol 2001;75:6450–6459. [PubMed: 11413312]

Amin R, Wilmott R, Schwarz Y, Trapnell B, Stark J. Replication-deficient adenovirus induces expression of interleukin-8 by airway epithelial cells in vitro. Hum Gene Ther 1995;6:145–153. [PubMed: 7734515]

Baggiolini M, Dewald B, Moser B. Interleukin-8 and related chemotactic cytokines—CXC and CC chemokines. Adv Immunol 1994;55:97–179. [PubMed: 8304236]

Ball AO, Williams ME, Spindler KR. Identification of mouse adenovirus type 1 early region 1: DNA sequence and a conserved transactivating function. J Virol 1988;62:3947–3957. [PubMed: 3172335]

Ball AO, Beard CW, Redick SD, Spindler KR. Genome organization of mouse adenovirus type 1 early region 1: a novel transcription map. Virology 1989;170:523–536. [PubMed: 2543128]

Ball AO, Beard CW, Villegas P, Spindler KR. Early region 4 sequence and biological comparison of two isolates of mouse adenovirus type 1. Virology 1991;180:257–265. [PubMed: 1845825]

Beard CW, Spindler KR. Characterization of an 11K protein produced by early region 3 of mouse adenovirus type 1. Virology 1995;208:457–466. [PubMed: 7747418]

Beard CW, Spindler KR. Analysis of early region 3 mutants of mouse adenovirus type 1. J Virol 1996;70:5867–5874. [PubMed: 8709206]

Beard CW, Ball AO, Wooley EH, Spindler KR. Transcription mapping of mouse adenovirus type 1 early region 3. Virology 1990;175:81–90. [PubMed: 2137954]

Becroft DM. Histopathology of fatal adenovirus infection of the respiratory tract in young children. J Clin Pathol 1967;20:561–569. [PubMed: 4301496]

Becroft DM. Bronchiolitis obliterans, bronchiectasis, and other sequelae of adenovirus type 21 infection in young children. J Clin Pathol 1971;24:72–82. [PubMed: 4324685]

Beeh KM, Kornmann O, Buhl R, Culpitt SV, Giembycz MA, Barnes PJ. Neutrophil chemotactic activity of sputum from patients with COPD: role of interleukin 8 and leukotriene B4. Chest 2003;123:1240–1247. [PubMed: 12684317]

Blease K, Lukacs NW, Hogaboam CM, Kunkel SL. Chemokines and their role in airway hyper-reactivity. Respir Res 2000;1:54–61. [PubMed: 11667966]

Booth JL, Coggeshall KM, Gordon BE, Metcalf JP. Adenovirus type 7 induces interleukin-8 in a lung slice model and requires activation of Erk. J Virol 2004;78:4156–4164. [PubMed: 15047831]

Carballal G, Videla C, Misirlian A, Requeijo PV, Aguilar Mdel C. Adenovirus type 7 associated with severe and fatal acute lower respiratory infections in Argentine children. BMC Pediatr 2002;2:6. [PubMed: 12184818]

Cauthen AN, Spindler KR. Sequence of the mouse adenovirus type-1 DNA encoding the 100-kDa, 33-kDa and DNA-binding proteins. Gene 1996;168:183–187. [PubMed: 8654941]

Cauthen, A.N., Spindler, K.R., 1999. Construction of mouse adenovirus type 1 mutants. In: Wold, W.S.M. (Ed.), Adenovirus Methods and Protocols. Humana Press, Totowa, NJ, pp. 85–103.

Cauthen AN, Brown CC, Spindler KR. In vitro and in vivo characterization of a mouse adenovirus type 1 early region 3 null mutant. J Virol 1999;73:8640–8646. [PubMed: 10482617]

Chany C, Lepine P, Lelong M, Le Tan V, Satge P, Virat J. Severe and fatal pneumonia in infants and young children associated with adenovirus infections. Am J Hyg 1958;67:367–378. [PubMed: 13533409]

Charles PC, Guida JD, Brosnan CF, Horwitz MS. Mouse adenovirus type-1 replication is restricted to vascular endothelium in the CNS of susceptible strains of mice. Virology 1998;245:216–228. [PubMed: 9636361]

Charles PC, Chen X, Horwitz MS, Brosnan CF. Differential chemokine induction by the mouse adenovirus type-1 in the central nervous system of susceptible and resistant strains of mice. J Neurovirol 1999;5:55–64. [PubMed: 10190691]

Dawson TC, Beck MA, Kuziel WA, Henderson F, Maeda N. Contrasting effects of CCR5 and CCR2 deficiency in the pulmonary inflammatory response to influenza A virus. Am J Pathol 2000;156:1951–1959. [PubMed: 10854218]

Domachowske JB, Bonville CA, Gao JL, Murphy PM, Easton AJ, Rosenberg HF. MIP-1 alpha is produced but it does not control pulmonary inflammation in response to respiratory syncytial virus infection in mice. Cell Immunol 2000;206:1–6. [PubMed: 11161432]

Edwards KM, Thompson J, Paolini J, Wright PF. Adenovirus infections in young children. Pediatrics 1985;76:420–424. [PubMed: 2993992]

Elliott WM, Hayashi S, Hogg JC. Immunodetection of adenoviral E1A proteins in human lung tissue. Am J Respir Cell Mol Biol 1995;12:642–648. [PubMed: 7766428]

Fang L, Stevens JL, Berk AJ, Spindler KR. Requirement of Sur2 for efficient replication of mouse adenovirus type 1. J Virol 2004;78:12888–12900. [PubMed: 15542641]

Ginsberg HS, Moldawer LL, Sehgal PB, Redington M, Kilian PL, Chanock RM, Prince GA. A mouse model for investigating the molecular pathogenesis of adenovirus pneumonia. Proc Natl Acad Sci USA 1991;88:1651–1655. [PubMed: 1848005]

Gottlieb K, Villarreal LP. The distribution and kinetics of polyomavirus in lungs of intranasally infected newborn mice. Virology 2000;266:52–65. [PubMed: 10612660]

Guida JD, Fejer G, Pirofski LA, Brosnan CF, Horwitz MS. Mouse adenovirus type 1 causes a fatal hemorrhagic encephalomyelitis in adult C57BL/6 but not BALB/c mice. J Virol 1995;69:7674–7681. [PubMed: 7494276]

Guo RF, Ward PA. Mediators and regulation of neutrophil accumulation in inflammatory responses in lung: insights from the IgG immune complex model. Free Radical Biol Med 2002;33:303–310. [PubMed: 12126752]

Haeberle HA, Kuziel WA, Dieterich HJ, Casola A, Gatalica Z, Garofalo RP. Inducible expression of inflammatory chemokines in respiratory syncytial virus-infected mice: role of MIP-1alpha in lung pathology. J Virol 2001;75:878–890. [PubMed: 11134301]

Harrod KS, Mounday AD, Stripp BR, Whitsett JA. Clara cell secretory protein decreases lung inflammation after acute virus infection. Am J Physiol 1998;275:L924–L930. [PubMed: 9815110]

Hobbs MV, Weigle WO, Noonan DJ, Torbett BE, McEvilly RJ, Koch RJ, Cardenas GJ, Ernst DN. Patterns of cytokine gene expression by $CD4^+$ T cells from young and old mice. J Immunol 1993;150:3602–3614. [PubMed: 8096853]

Hogaboam CM, Steinhauser ML, Schock H, Lukacs N, Strieter RM, Standiford T, Kunkel SL. Therapeutic effects of nitric oxide inhibition during experimental fecal peritonitis: role of interleukin-10 and monocyte chemoattractant protein 1. Infect Immun 1998;66:650–655. [PubMed: 9453622]

Hogg JC. Childhood viral infection and the pathogenesis of asthma and chronic obstructive lung disease. Am J Respir Crit Care Med 1999;160:S26–S28. [PubMed: 10556165]

Hogg JC. Role of latent viral infections in chronic obstructive pulmonary disease and asthma. Am J Respir Crit Care Med 2001;164:S71–S75. [PubMed: 11734471]

Horwitz, M.S., 2001. Adenoviruses. In: Knipe, D.M., Howley, P.M. (Eds.), Fields Virology, vol. 2. Lippincott Williams and Wilkins, Philadelphia, pp. 2301–2327.

Huebner RJ, Rowe WP, Chanock RM. Newly recognized respiratory tract viruses. Annu Rev Microbiol 1958;12:49–76. [PubMed: 13595601]

John AE, Berlin AA, Lukacs NW. Respiratory syncytial virus-induced CCL5/RANTES contributes to exacerbation of allergic airway inflammation. Eur J Immunol 2003;33:1677–1685. [PubMed: 12778486]

Kajon AE, Brown CC, Spindler KR. Distribution of mouse adenovirus type 1 in intraperitoneally and intranasally infected adult outbred mice. J Virol 1998;72:1219–1223. [PubMed: 9445021]

Kajon AE, Gigliotti AP, Harrod KS. Acute inflammatory response and remodeling of airway epithelium after subspecies B1 human adenovirus infection of the mouse lower respiratory tract. J Med Virol 2003;71:233–244. [PubMed: 12938198]

Kay MA, Glorioso JC, Naldini L. Viral vectors for gene therapy: the art of turning infectious agents into vehicles of therapeutics. Nat Med 2001;7:33–40. [PubMed: 11135613]

Kodama Y, Setoguchi Y, Fukuchi Y. Infection of replication-deficient adenoviral vector enhances interleukin-8 production in small airway epithelial cells more than in large airway epithelial cells. Respirology 2001;6:271–279. [PubMed: 11844116]

Kojaoghlanian T, Flomenberg P, Horwitz MS. The impact of adenovirus infection on the immunocompromised host. Rev Med Virol 2003;13:155–171. [PubMed: 12740831]

Kolavic-Gray SA, Binn LN, Sanchez JL, Cersovsky SB, Polyak CS, Mitchell-Raymundo F, Asher LV, Vaughn DW, Feighner BH, Innis BL. Large epidemic of adenovirus type 4 infection among military trainees: epidemiological, clinical, and laboratory studies. Clin Infect Dis 2002;35:808–818. [PubMed: 12228817]

Kring SC, Spindler KR. Sequence of mouse adenovirus type 1 DNA encoding the amino terminus of protein IVa2. Nucleic Acids Res 1990;18:4003. [PubMed: 2374728]

Kring SC, Ball AO, Spindler KR. Transcription mapping of mouse adenovirus type 1 early region 4. Virology 1992;190:248–255. [PubMed: 1388309]

Kring SC, King CS, Spindler KR. Susceptibility and signs associated with mouse adenovirus type 1 infection of adult outbred Swiss mice. J Virol 1995;69:8084–8088. [PubMed: 7494327]

Larranaga C, Kajon A, Villagra E, Avendano LF. Adenovirus surveillance on children hospitalized for acute lower respiratory infections in Chile (1988–1996). J Med Virol 2000;60:342–346. [PubMed: 10630968]

Leland Booth J, Metcalf JP. Type-specific induction of interleukin-8 by adenovirus. Am J Respir Cell Mol Biol 1999;21:521–527. [PubMed: 10502562]

Liu Q, Muruve DA. Molecular basis of the inflammatory response to adenovirus vectors. Gene Ther 2003;10:935–940. [PubMed: 12756413]

Lukacs NW. Role of chemokines in the pathogenesis of asthma. Nat Rev, Immunol 2001;1:108–116. [PubMed: 11905818]

Luster AD. Chemokines—Chemotactic cytokines that mediate inflammation. N Engl J Med 1998;338:436–445. [PubMed: 9459648]

Macek V, Sorli J, Kopriva S, Marin J. Persistent adenoviral infection and chronic airway obstruction in children. Am J Respir Crit Care Med 1994;150:7–10. [PubMed: 8025775]

Marin J, Jeler-Kacar D, Levstek V, Macek V. Persistence of viruses in upper respiratory tract of children with asthma. J Infect 2000;41:69–72. [PubMed: 10942643]

Matsuse T, Hayashi S, Kuwano K, Keunecke H, Jefferies WA, Hogg JC. Latent adenoviral infection in the pathogenesis of chronic airways obstruction. Am Rev Respir Dis 1992;146:177–184. [PubMed: 1626800]

Meissner JD, Hirsch GN, LaRue EA, Fulcher RA, Spindler KR. Completion of the DNA sequence of mouse adenovirus type 1: sequence of E2B, L1, and L2 (18–51 map units). Virus Res 1997;51:53–64. [PubMed: 9381795]

Mejias A, Chavez-Bueno S, Rios AM, Saavedra-Lozano J, Fonseca Aten M, Hatfield J, Kapur P, Gomez AM, Jafri HS, Ramilo O. Anti-respiratory syncytial virus (RSV) neutralizing antibody decreases lung inflammation, airway obstruction, and airway hyper-responsiveness in a murine RSV model. Antimicrob Agents Chemother 2004;48:1811–1822. [PubMed: 15105140]

Meshi B, Vitalis TZ, Ionescu D, Elliott WM, Liu C, Wang XD, Hayashi S, Hogg JC. Emphysematous lung destruction by cigarette smoke. The effects of latent adenoviral infection on the lung inflammatory response. Am J Respir Cell Mol Biol 2002;26:52–57. [PubMed: 11751203]

Miller AL, Bowlin TL, Lukacs NW. Respiratory syncytial virus-induced chemokine production: linking viral replication to chemokine production in vitro and in vivo. J Infect Dis 2004;189:1419–1430. [PubMed: 15073679]

Mogabgab WJ. Mycoplasma pneumoniae and adenovirus respiratory illnesses in military and university personnel, 1959–1966. Am Rev Respir Dis 1968;97:345–358. [PubMed: 4295592]

Moore ML, Brown CC, Spindler KR. T cells cause acute immunopathology and are required for long-term survival in mouse adenovirus type 1-induced encephalomyelitis. J Virol 2003;77:10060–10070. [PubMed: 12941916]

Noah TL, Wortman IA, Hu PC, Leigh MW, Boucher RC. Cytokine production by cultured human bronchial epithelial cells infected with a replication-deficient adenoviral gene transfer vector or wild-type adenovirus type 5. Am J Respir Cell Mol Biol 1996;14:417–424. [PubMed: 8624246]

Otake K, Ennist DL, Harrod K, Trapnell BC. Nonspecific inflammation inhibits adenovirus-mediated pulmonary gene transfer and expression independent of specific acquired immune responses. Hum Gene Ther 1998;9:2207–2222. [PubMed: 9794205]

Pacini DL, Dubovi EJ, Clyde WA Jr. A new animal model for human respiratory tract disease due to adenovirus. J Infect Dis 1984;150:92–97. [PubMed: 6086773]

Pacini DL, Collier AM, Henderson FW. Adenovirus infections and respiratory illnesses in children in group day care. J Infect Dis 1987;156:920–927. [PubMed: 2824627]

Power UF, Huss T, Michaud V, Plotnicky-Gilquin H, Bonnefoy JY, Nguyen TN. Differential histopathology and chemokine gene expression in lung tissues following respiratory syncytial virus (RSV) challenge of formalin-inactivated RSV- or BBG2Na-immunized mice. J Virol 2001;75:12421–12430. [PubMed: 11711632]

Prince GA, Porter DD, Jenson AB, Horswood RL, Chanock RM, Ginsberg HS. Pathogenesis of adenovirus type 5 pneumonia in cotton rats (*Sigmodon hispidus*). J Virol 1993;67:101–111. [PubMed: 8380066]

Qiu Y, Zhu J, Bandi V, Atmar RL, Hattotuwa K, Guntupalli KK, Jeffery PK. Biopsy neutrophilia, neutrophil chemokine and receptor gene expression in severe exacerbations of chronic obstructive pulmonary disease. Am J Respir Crit Care Med 2003;168:968–975. [PubMed: 12857718]

Rochford R, Lutzke ML, Alfinito RS, Clavo A, Cardin RD. Kinetics of murine gammaherpesvirus 68 gene expression following infection of murine cells in culture and in mice. J Virol 2001;75:4955–4963. [PubMed: 11333874]

Rollins BJ. Chemokines. Blood 1997;90:909–928. [PubMed: 9242519]

Saetta M, Mariani M, Panina-Bordignon P, Turato G, Buonsanti C, Baraldo S, Bellettato CM, Papi A, Corbetta L, Zuin R, Sinigaglia F, Fabbri LM. Increased expression of the chemokine receptor CXCR3 and its ligand CXCL10 in peripheral airways of smokers with chronic obstructive pulmonary disease. Am J Respir Crit Care Med 2002;165:1404–1409. [PubMed: 12016104]

Sarawar SR, Lee BJ, Anderson M, Teng YC, Zuberi R, Von Gesjen S. Chemokine induction and leukocyte trafficking to the lungs during murine gammaherpesvirus 68 (MHV-68) infection. Virology 2002;293:54–62. [PubMed: 11853399]

Schwarz YA, Amin RS, Stark JM, Trapnell BC, Wilmott RW. Interleukin-1 receptor antagonist inhibits interleukin-8 expression in A549 respiratory epithelial cells infected in vitro with a replication-deficient recombinant adenovirus vector. Am J Respir Cell Mol Biol 1999;21:388–394. [PubMed: 10460756]

Smith, K., Spindler, K.R., 1999. Murine adenovirus. In: Ahmed, R., Chen, I. (Eds.), Persistent Viral Infections. John Wiley and Sons, Ltd., pp. 477–484.

Smith K, Ying B, Ball AO, Beard CW, Spindler KR. Interaction of mouse adenovirus type 1 early region 1A protein with cellular proteins pRb and p107. Virology 1996;224:184–197. [PubMed: 8862413]

Smith K, Brown CC, Spindler KR. The role of mouse adenovirus type 1 early region 1A in acute and persistent infections in mice. J Virol 1998;72:5699–5706. [PubMed: 9621028]

Spindler KR, Fang L, Moore ML, Hirsch GN, Brown CC, Kajon A. SJL/J mice are highly susceptible to infection by mouse adenovirus type 1. J Virol 2001;75:12039–12046. [PubMed: 11711594]

Taub DD. Chemokine–leukocyte interactions. The voodoo that they do so well. Cytokine Growth Factor Rev 1996;7:355–376. [PubMed: 9023058]

Tekkanat KK, Maassab H, Miller A, Berlin AA, Kunkel SL, Lukacs NW. RANTES (CCL5) production during primary respiratory syncytial virus infection exacerbates airway disease. Eur J Immunol 2002;32:3276–3284. [PubMed: 12555673]

Traves SL, Culpitt SV, Russell RE, Barnes PJ, Donnelly LE. Increased levels of the chemokines GROalpha and MCP-1 in sputum samples from patients with COPD. Thorax 2002;57:590–595. [PubMed: 12096201]

Tumpey TM, Lu X, Morken T, Zaki SR, Katz JM. Depletion of lymphocytes and diminished cytokine production in mice infected with a highly virulent influenza A (H5N1) virus isolated from humans. J Virol 2000;74:6105–6116. [PubMed: 10846094]

van der Veen J, Mes A. Experimental infection with mouse adenovirus in adult mice. Arch Gesamte Virusforsch 1973;42:235–241. [PubMed: 4356771]

Vitalis TZ, Keicho N, Itabashi S, Hayashi S, Hogg JC. A model of latent adenovirus 5 infection in the guinea pig (*Cavia porcellus*). Am J Respir Cell Mol Biol 1996;14:225–231. [PubMed: 8845172]

Vitalis TZ, Kern I, Croome A, Behzad H, Hayashi S, Hogg JC. The effect of latent adenovirus 5 infection on cigarette smoke-induced lung inflammation. Eur Respir J 1998;11:664–669. [PubMed: 9596119]

Walley KR, Lukacs NW, Standiford TJ, Strieter RM, Kunkel SL. Elevated levels of macrophage inflammatory protein 2 in severe murine peritonitis increase neutrophil recruitment and mortality. Infect Immun 1997;65:3847–3851. [PubMed: 9284162]

Weinberg JB, Lutzke ML, Efstathiou S, Kunkel S, Rochford R. Elevated chemokine responses are maintained in lungs after clearance of viral infection. J Virol 2002;76:10518–10523. [PubMed: 12239330]

Weinberg JB, Lutzke ML, Alfinito R, Rochford R. Mouse strain differences in the chemokine response to acute lung infection with a murine gammaherpesvirus. Viral Immunol 2004;17:69–77. [PubMed: 15018663]

Wigand R. Age and susceptibility of Swiss mice for mouse adenovirus, strain FL. Arch Virol 1980;64:349–357. [PubMed: 6249244]

Wigand R, Gelderblom H, Ozel M. Biological and biophysical characteristics of mouse adenovirus, strain FL. Arch Virol 1977;54:131–142. [PubMed: 560839]

Yamada K, Elliott WM, Hayashi S, Brattsand R, Roberts C, Vitalis TZ, Hogg JC. Latent adenoviral infection modifies the steroid response in allergic lung inflammation. J Allergy Clin Immunol 2000;106:844–851. [PubMed: 11080705]

Yamada K, Elliott WM, Brattsand R, Valeur A, Hogg JC, Hayashi S. Molecular mechanisms of decreased steroid responsiveness induced by latent adenoviral infection in allergic lung inflammation. J Allergy Clin Immunol 2002;109:35–42. [PubMed: 11799363]

Zahradnik JM, Spencer MJ, Porter DD. Adenovirus infection in the immunocompromised patient. Am J Med 1980;68:725–732. [PubMed: 6246799]

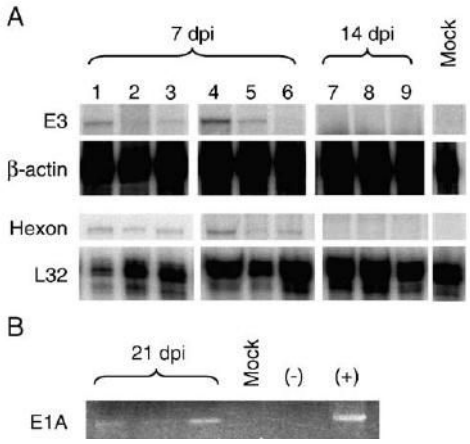

Fig. 1.

Detection of MAV-1 gene expression and DNA in lung. (A) RNA was obtained from the lungs of mice infected i.n. with 10^5 PFU of MAV-1-or mock-infected with conditioned media. RNA was analyzed using RPA to detect expression of the MAV-1 E3 and hexon genes and the GAPDH and L32 mouse housekeeping genes. Protected viral probe fragments are shown from RNA isolated from mouse lungs at 7 and 14 dpi. Lanes 1 to 3 present data for individual mice from one experiment at 7 dpi, and lanes 4 to 9 present data for individual mice from a separate experiment at 7 and 14 dpi. (B) DNA was obtained from lungs harvested from infected and mock-infected mice at 21 dpi. PCR was used to amplify a segment of the MAV-1 E1A gene. β-actin was successfully amplified from every sample as a control (data not shown).

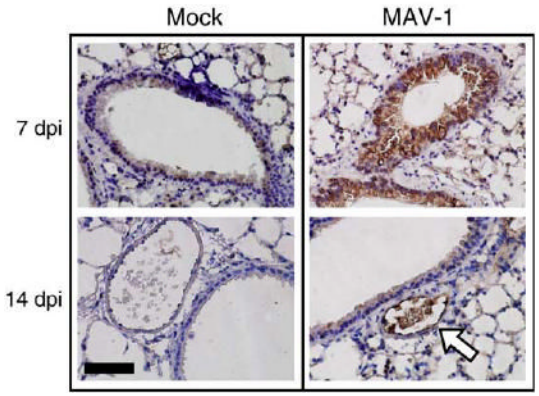

Fig. 2.

Localization of MAV-1 in lung. Immunohistochemistry was performed on paraffin-embedded sections from the lungs of mice infected i.n. with 10^5 PFU of MAV-1- or mock-infected with conditioned media. Polyclonal rabbit antiserum was used to detect MAV-1 E3 protein at 7 and 14 dpi. Staining of mock-infected lungs is shown for comparison. Dark brown staining indicates virus-specific staining, which is present in respiratory epithelial cells at 7 dpi. Open arrow indicates virus-specific staining of vascular endothelial cells at 14 dpi. Scale bar, 100 μm.

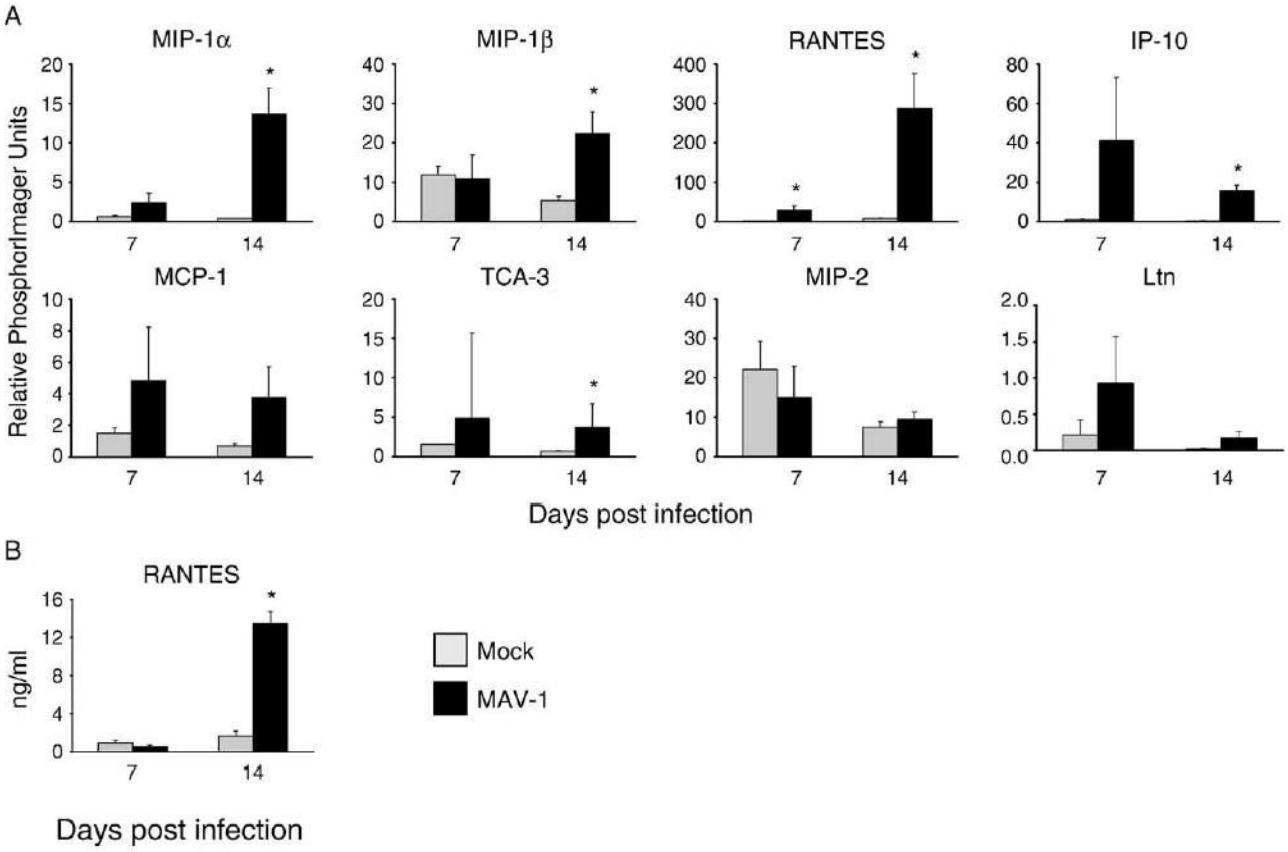

Fig. 3.

Chemokine responses to MAV-1 in the lung. (A) RPA measurement of chemokine gene expression at the indicated time points in the lungs of mice infected i.n. with 10^5 PFU of MAV-1 or mock-infected with conditioned media. Quantified data are presented as percentages of the expression of the L32 housekeeping gene. (B) ELISA measurement of protein levels of the representative CC chemokine RANTES in the lungs of MAV-1-infected and mock-infected mice. For both RPA and ELISA, data are presented as means ± standard deviation of values obtained from three mice at each condition (except mock infection at 7 dpi, where $n = 2$) from one representative experiment corresponding to lanes 4 to 9 in Fig. 1. Statistical significance was determined using Student's *t* test (*$P < 0.05$). Similar results were obtained from a separate independent experiment.

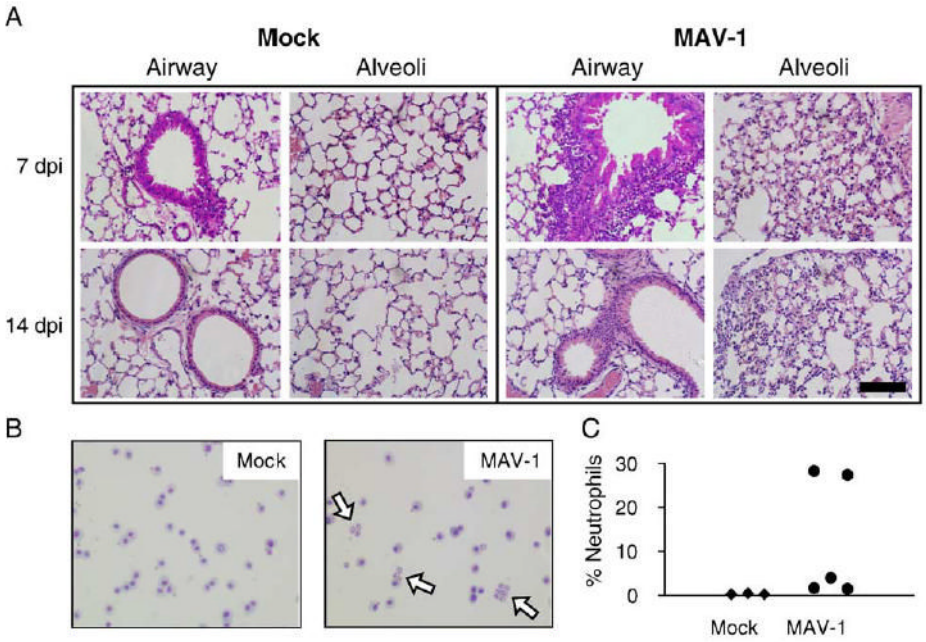

Fig. 4.

Cellular inflammatory responses to MAV-1 respiratory infection. (A) Hematoxylin and eosin-stained sections of lungs of MAV-1-infected and mock-infected mice demonstrate a mononuclear cellular infiltrate surrounding airways that is most prominent at 7 dpi and a mild interstitial pneumonitis that is present at both 7 and 14 dpi. Scale bar, 100 μm. (B) Hematoxylin and eosin-stained cytospins of BAL fluid demonstrate an increased number of neutrophils (open arrows) in the airways of MAV-1-infected mice at 7 dpi. (C) Neutrophils as a percentage of all cells in bronchoalveolar lavage fluid collected from mock-infected (n = 3) and MAV-1-infected (n = 5) mice at 7 dpi. Each symbol represents an individual mouse.